GEOFLUIDS
Geofluids (2011) **11**, 134–143 doi: 10.1111/j.1468-8123.2011.00325.x

High-temperature magmatic fluid exsolved from magma at the Duobuza porphyry copper–gold deposit, Northern Tibet

J. X. LI, G. M. LI, K. Z. QIN AND B. XIAO

Key Laboratory of Mineral Resources, Institute of Geology and Geophysics, Chinese Academy of Sciences, Beijing, China

ABSTRACT

The Duobuza porphyry copper–gold deposit (proven Cu resources of 2.7 Mt, 0.94% Cu and 13 t gold, 0.21 g t^{-1} Au) is located at the northern margin of the Bangong-Nujiang suture zone separating the Qiangtang and Lhasa Terranes. The major ore-bearing porphyry consists of granodiorite. The alteration zone extends from silicification and potassic alteration close to the porphyry stock to moderate argillic alteration and propylitization further out. Phyllic alteration is not well developed. Sericite-quartz veins only occur locally. High-temperature, high-salinity fluid inclusions were observed in quartz phenocrysts and various quartz veins. These fluid inclusions are characterized by sylvite dissolution between 180 and 360°C and halite dissolution between 240 and 540°C, followed by homogenization through vapor disappearance between 620 and 960°C. Daughter minerals were identified by SEM as chalcopyrite, halite, sylvite, rutile, K–feldspar, and Fe–Mn-chloride. They indicate that the fluid is rich in ore-forming elements and of high oxidation state. The fluid belongs to a complex hydrothermal system containing H_2O – NaCl – KCl ± $FeCl_2$ ± $CaCl_2$ ± $MnCl_2$. With decreasing homogenization temperature, the fluid salinity tends to increase from 34 to 82 wt% NaCl equiv., possibly suggesting a pressure or Cl/H_2O increase in the original magma. No coexisting vapor-rich fluid inclusions with similar homogenization temperatures were found, so the brines are interpreted to have formed by direct exsolution from magma rather than trough boiling off of a low-salinity vapor. Estimated minimum pressure of 160 MPa imply approximately 7-km depth. This indicates that the deposit represents an orthomagmatic end member of the porphyry copper deposit continuum. Two key factors are proposed for the fluid evolution responsible for the large size of the gold-rich porphyry copper deposit of Duobuza: (i) ore-forming fluids separated early from the magma, and (ii) the hydrothermal fluid system was of magmatic origin and highly oxidized.

Key words: Duobuza, High-temperature and high-salinity primary magmatic fluid, Northern Tibet, orthomagmatic model, porphyry copper–gold deposit

Received 5 May 2010; accepted 3 January 2011

Corresponding author: Jinxiang Li, Key Laboratory of Mineral Resources, Institute of Geology and Geophysics, Chinese Academy of Sciences, Beijing, China.
Email: ljx@mail.iggcas.ac.cn. Tel.: 86 10 82998187. Fax: 86 10 62010846.

Geofluids (2011) **11**, 134–143

INTRODUCTION

The study of fluid inclusions in porphyry Cu (±Mo ± Au) deposits is an effective tool to trace the ore-forming process (Roedder 1984; Bodnar 1995; Heinrich *et al.* 2005, Heinrich 2007). Fluid exsolution from hydrous magma plays an important role in mineralization (Hedenquist & Lowenstern 1994; Webster 1997; Audétat & Pettke 2003; Imai 2005; Kamenetsky & Kamenetsky 2010), and early fluid exsolution is favorable for economic mineralization because it favors the transfer of ore-forming elements into the fluid (Candela & Holland 1986; Zhang *et al.* 2001; Li *et al.* 2006). Commonly, a relatively low-salinity fluid exsolves from the magma. Because of the decompression, the fluid unmixes ('boils') and produces a high-salinity brine and a vapor-rich fluid. At lower temperature, liquid-rich inclusion of lower salinity can be produced by meteoric water addition and dilution (Hedenquist *et al.* 1998; Li *et al.* 2006, 2007). However, the time and pressure of the initial fluid exsolution from the magma and the transition from the magmatic to the hydrothermal stage remain unclear.

© 2011 Blackwell Publishing Ltd

Petrographic study of the Duobuza porphyry copper–gold deposit has shown abundant fluid inclusions. The characteristics and evolution of fluids below ~600°C have been systematically studied by She *et al.* (2006) and Li *et al.* (2007). In this study, we focus on magmatic fluid inclusions of higher temperature and high salinity discovered in the Duobuza porphyry copper–gold deposit. Through the study of these inclusions, we explore the initial time, pressure, and mechanism of fluid exsolution from the magma and the magmatic-hydrothermal evolution contributing to porphyry copper–gold mineralization.

GEOLOGIC SETTING OF THE DUOBUZA DEPOSIT

The Duobuza porphyry copper–gold deposit was discovered by No.5 Geological Team, Tibet Bureau of Geology and Exploration in 2000. It has now been confirmed to be a high-grade and world-class deposit. The ore district is located 100 km northwest of Gerze country. It was found between the southern edge of the Qiangtang block and the northern margin of the Bangong-Nujiang suture zone (Fig. 1A). The geochemical characteristics of the magmatic rocks indicate that the deposit was formed in a continental arc setting (Li *et al.* 2008b). The Duobuza porphyry copper–gold deposit is located at the NWW margin of a large circular structure in an east–west trending uplifted block of ~30 km length and ~10 km width. The stratigraphy is mainly made up of the Middle Jurassic Yanshiping group, the Late Cretaceous Meiriqie group (K_1m), the Early Tertiary Kangtuo group (N_1k), and partial Quaternary cover (Fig. 1B). The Middle Jurassic Yanshiping group shows an interbedded volcanoclastic to littoral facies distribution with EW trending extension, 50°–80° dipping toward NWW, and it consists of arkose and siltstone interbedded with basalt and dacite. The Late Cretaceous Meiriqie group contains volcanoclastic andesite rich in plagioclase and amphibole phenocrysts.

Mafic to intermediate hypabyssal rocks intruded the Middle Jurassic Yanshiping group strata. They mainly comprise gabbro, diabase porphyry, diorite, quartz diorite, quartz diorite porphyry, granodiorite porphyry, and mostly appear as stocks and dykes. The granodioritic porphyry stock is the main ore-bearing intrusion. The intrusion is partly exposed as an elongated band (200 × 1000 m) in the northeastern part of the ore district and in the

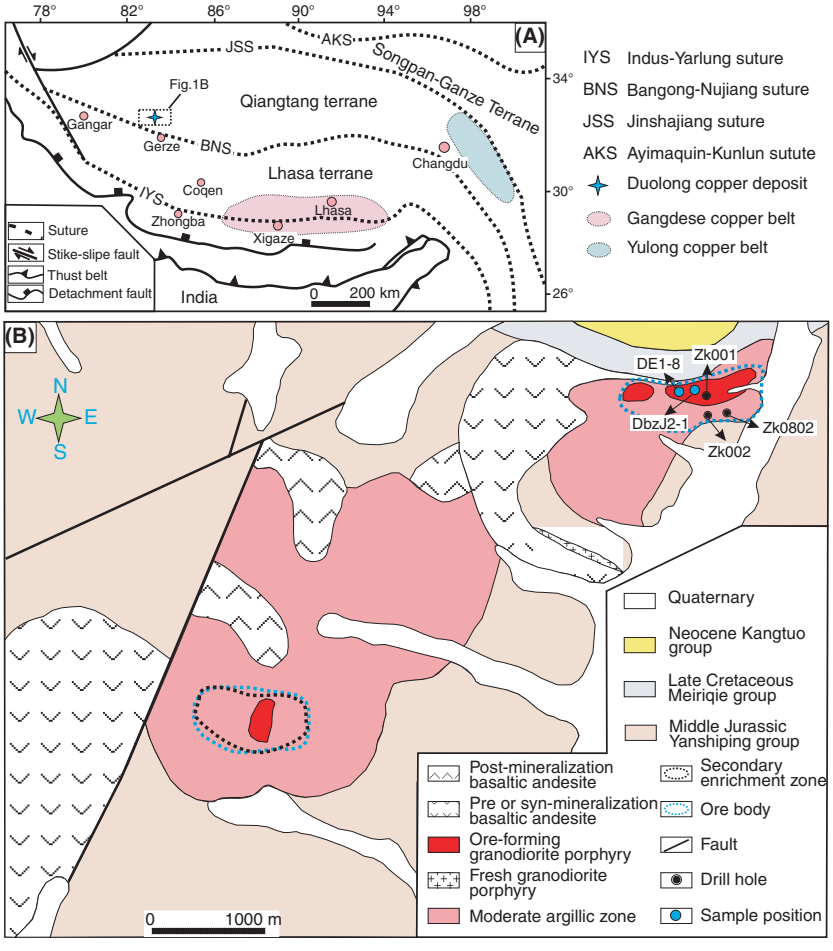

Fig. 1. Tectonic and location map (A, after Hou *et al.* 2004) and generalized geological map of the Duobuza porphyry copper–gold district in the Bangonghu tectonic belt (B, after Li 2008a).

southwestern part as an elliptical outcrop (300 × 200 m), with mineralization extending over an area of 1400 × 500 m (Fig. 1B). On the basis of the alteration characteristics, the volcanic rocks can be divided into pre-, syn-, and postmineralization basaltic andesites (Fig. 1B). The ore-bearing granodiorite porphyry intruded the basaltic andesite and was responsible for its propylitic alteration. The geochemical characteristics of the porphyries and all volcanic rocks show that they have the characteristics of arc magmas (Li *et al.* 2008b): a high-K, calc-alkaline series depleted in HFSE (such as Nb, Ta, Zr and Hf) and enriched in large ion lithophile elements such as Rb and Ba, ranging from basaltic rocks (SiO_2 49–53%) to granodioritic composition (SiO_2 65–68%). The SHRIMP zircon U-Pb age of the ore-bearing granodiorite porphyry is 121.6 ± 1.9 Ma (Li *et al.* 2008b), indicating that this deposit formed in the Early Cretaceous as a result of the subduction of the Neo-Tethys Ocean (Mo & Pan 2006; Shi 2007).

Hydrothermal alterations and veinlet characteristics

The emplacement of the granodiorite porphyry stock was responsible for a wide range of hydrothermal alteration. Detailed mapping revealed albitization, biotitization, sericitization, silicification, epidotization, chloritization, carbonatization, illitization, and kaolinization. The area of alteration spreads more than 10 km^2. The main wall rock alteration zones extending outward from the ore-bearing porphyry center can be divided into potassic alteration, partly superimposed moderate argillic alteration and adjacent propylitization (Fig. 2). Phyllic alteration is not well developed, and sericite-quartz veins only occur locally. Hydrothermal magnetite is abundant and occurs in consistent association with copper sulfides and gold.

Micro-fractures and fissures are well developed within the deposit. Their exceptionally high frequency is between 60 and 500 per meter, but a mean range is between 95 and 350 per meter. Fissure and veinlet frequency correlate with high ore grades. A series of thicker veins (0.5–1.5 cm) developed concurrently (Li *et al.* 2007; Li 2008a). On the basis of mineralogy and cross-cutting relationships, we classified several vein types into three main stages (Table 1). Stage 1: biotite veins (corresponding to the EB type of Gustafson & Quiroga 1995), K-feldspar – biotite – chalcopyrite – quartz veins, quartz – chalcopyrite – magnetite veins (A-type, Gustafson & Hunt 1975), and quartz – magnetite – biotite – K-feldspar veins, all in potassic alteration zone; Stage 2: quartz – chalcopyrite veins with chalcopyrite occurring in the center of the vein (B-type, Gustafson & Hunt 1975), quartz – chalcopyrite – pyrite veins, quartz – pyrite veins, quartz – molybdenite – chalcopyrite veins in the moderate argillic alteration zone; Stage 3: gypsum veins, quartz – pyrite veins, gypsum – chalcopyrite veins and calcite veins in the wall rock.

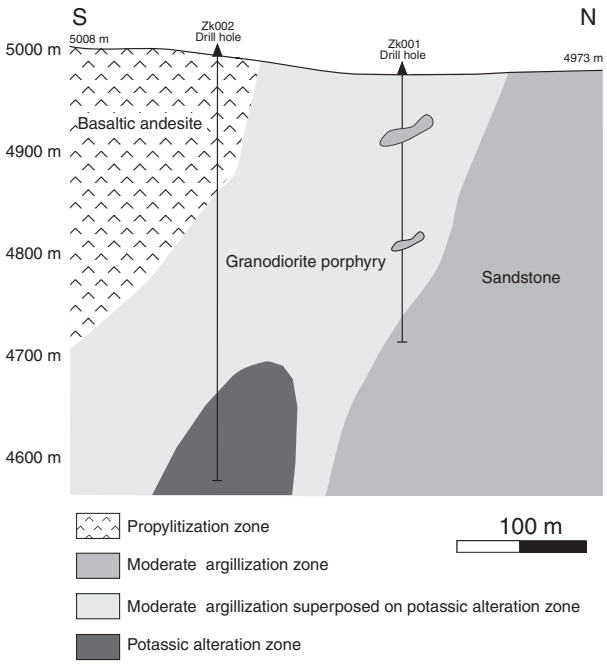

Fig. 2. The cross-section of Duobuza porphyry copper–gold deposit, Tibet (modified from Li *et al.* 2007).

Mineralization characteristics

The northern ore segment of the Duobuza ore district occurs in the granodiorite porphyry, in its contact zone with wall rocks, and in the potassic and superimposed moderate argillic alteration zones. The orebody has been defined over a width of 100~400 m in north–south direction, an east–west strike length of 1400 m, a vertical extent of about 500 m from outcrop, and it dips between 65° and 80° toward 200°. The proven metal resource is of 2.7 million tons Cu with grade of 0.94% and 13 tons Au with 0.21 g t^{-1}, but prospective resources may extend to 4–5 Mt Cu and 30–50 t Au (unpublished report by No.5 Geological Team, Tibet Bureau of Geology and Exploration in 2003). Microscopic petrography indicates that copper and gold mineralization dominantly occurred in the early potassic alteration stage. Main hypogene ore minerals are chalcopyrite and magnetite, followed by pyrite, hematite, rutile, minor chalcocite, bornite, and native gold. The amount of chalcopyrite is greater than bornite, and both exceed pyrite. Gangue minerals are K-feldspar, albite, quartz, sericite, chlorite, carbonate, illite, and gypsum. Only one small molybdenite – quartz vein was identified. Vertical gradients in mineralization are as follows: stockwork veinlets and disseminated copper decrease from the upper part of the ore body to depth. Preliminary analysis revealed that there is a positive correlation between gold and copper (Li *et al.* 2007), without any systematic variation in Cu/Au ratio with depth. A secondary enrichment zone of 70–100 m thickness (Fig. 1B) was defined

Table 1 Characteristics of various veinlets (from early to late) in the Duobuza porphyry copper–gold deposit.

Veinlet type	Distribution	Shape	Width (mm)	Minerals amount (%)	Alteration zone
Q-Mt-Cp veinlet (A type, Gustafson & Hunt 1975)	Dominate in the ore-forming granodiorite porphyry	Irregular	5–10	Q (60–90), Mt (5–20), Cp (5–20)	Potassic
Q-Mt ± Bio ± Kfs ± Cp veinlet		Irregular	0.5–5	Q (50–70), Bio (5–10), Kfs (10–15) Mt (5–10), Cp (10–15)	
Q-Mt veinlet		Irregular	5–10	Q (80–90), Mt (10–20)	
Bio veinlet (EB type, Gustafson & Quiroga 1995)		Irregular	1–2	Bio (90–100), Mt (0–5), Cp (0–5)	
Kfs veinlet		Irregular	3–5	Kfs (90–95), Q (5–10)	
Q-Cp veinlet (B type, Gustafson & Hunt 1975)		Flat	5–20	Q (70–80), Cp (20–30)	
Q-Cp-Mo veinlet	In the ore-forming granodiorite porphyry and wall rock	Flat	2–10	Q (60–70), Cp (15–20), Mo (15-20)	Moderate argillization
Q-Cp-Py veinlet		Flat	2–10	Q (50–70), Cp (10–15), Py (20–35)	
Q-Ser veinlet	Dominate in the wall rock, less in the ore-forming granodiorite porphyry	Irregular	2	Q (50–70), Ser (20–30), Py (10–20)	
Q-Py veinlet (D type, Gustafson & Hunt 1975)		Flat	5–10	Q (70–80), Py (20–30)	
Gy veinlet	In the ore-forming granodiorite porphyry and wall rock	Irregular	0.1–2	Gp (90–100), Cal (0–10)	Moderate argillization and propylitization
Gy-Cp ± Py veinlet		Irregular	5–6	Gp (60–80), Cp (5–10), Py (15–30)	
Cal veinlet	Dominate in the wall rock	Irregular	20	Cal (100)	

Q, Quartz; Kfs, K-feldspar; Bio, Biotite; Chl, Chlorite; Gp, Gypsum; Cal, Calcite; Mt, Magnetite; Rut, Rutile; Hem, Hematite; Cp, Chalcopyrite; Bn, Bornite; Mo, Molybdenite; Py, Pyrite.

surrounding the southwestern part of the deposit. Its average copper grade is higher than 1.17%, and its average gold grade is 0.28 g t^{-1}. Ore minerals are malachite, azurite, limonite, chalcocite, native copper, and cuprite.

SUMMARY OF INTERMEDIATE-TO-LOW TEMPERATURE FLUID INCLUSIONS

The intermediate to low-temperature fluid inclusions in the Duobuza porphyry copper–gold deposit were studied in detail by Li *et al.* (2007). According to the phase relations at room temperature and the characteristics of phase transition upon heating, fluid inclusions in quartz phenocrysts and quartz-bearing veins (A type, B type and others; Table 1) are divided into three types: liquid-rich inclusions, vapor-rich inclusions, and multiphase brine inclusions. Vapor-rich inclusions are interpreted to be coeval with multiphase brine inclusions or abundant liquid-rich inclusions, indicating that the ore-forming fluid was boiling (Li *et al.* 2007).

Homogenization temperatures of fluid inclusions varied from 130 to 600°C (Li *et al.* 2007). The bulk of liquid-rich inclusions was homogenized below 350°C by vapor phase disappearance. Multiphase brine and vapor-rich inclusions were homogenized between 350 and 600°C. Vapor-rich inclusions were homogenized by liquid disappearance, and multiphase brine fluid inclusions were homogenized by halite dissolution or vapor disappearance (Li *et al.* 2007). The salinity of fluid inclusions varies from 0.8 wt% NaCl equiv. to 82 wt% NaCl + KCl equiv. and can be divided into three salinity ranges (Li *et al.* 2007): a low-salinity range of <20 wt% NaCl equiv. for liquid- and vapor-rich inclusions; a high-salinity range of 30–60 wt% NaCl equiv. for halite-bearing vapor-rich inclusions and multiphase brine inclusions; and an ultra-high salinity range of 60–82 wt% NaCl + KCl equiv. for multiphase brine inclusions.

Ore-forming fluid was separated into a low-salinity vapor and a high-salinity multiphase brine because of boiling between 400 and 600°C. Both inclusion types were possibly trapped at estimated pressures between 30 and 80 MPa (Li *et al.* 2007). Halite-bearing vapor-rich inclusions with salinities of 30–40 wt% NaCl equiv. may have formed from a fluid that exsolved directly from the magma. Liquid-rich inclusions with homogenization temperatures from 130 to 400°C and a salinity range from 0.7 to 22 wt% NaCl equiv. may be the result of vapor phase contraction (Heinrich *et al.* 2004; Li *et al.* 2007). The corresponding O and H stable isotope data indicate a dominantly magmatic source (Li 2008a).

HIGH-TEMPERATURE AND HIGH-SALINITY FLUID INCLUSIONS

Sample description and methods

We studied fluid inclusions in quartz phenocrystals and quartz veins of ore-forming porphyric and wall rock samples (Table 1), collected from outcrops and drill cores intersecting the northeastern partition of the Duobuza copper deposit (Figs 1B and 3; Table 2). Over 50 samples were studied for inclusion type, abundance, and their

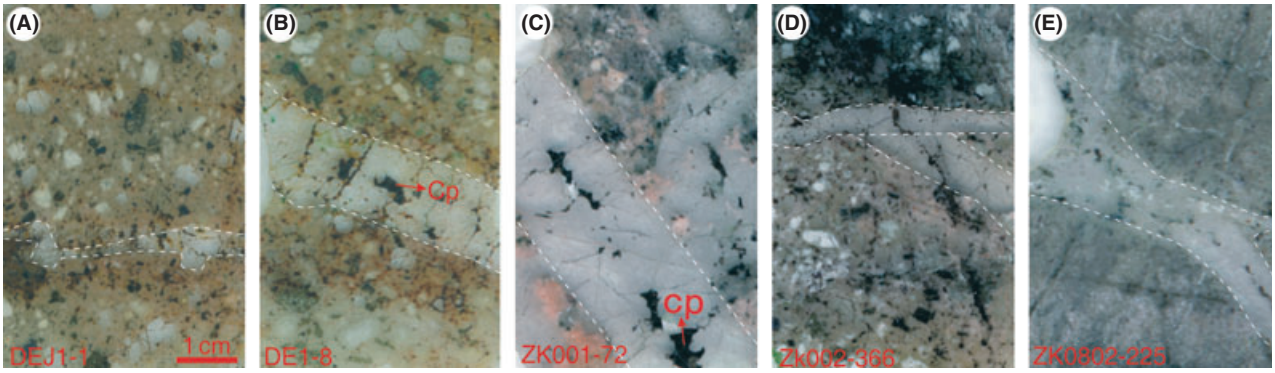

Fig. 3. Fluid inclusions section of hosting high-temperature and salinity fluid inclusions. (A) Argillization-silication granodiorite porphyry and developing quartz-chalcopyrite (Cp) vein with irregular vein wall; (B) Silicification-argillization granodiorite porphyry and developing quartz-chalcopyrite vein with straight vein wall; (C) potassic-argillization granodiorite porphyry and developing B-type vein; (D) potassic-argillization granodiorite porphyry and developing A-type vein; (E) silicification-chloritization wall rock (basaltic-andesitic volcanic rocks) and developing quartz-chalcopyrite vein.

Table 2 Characteristics of high-temperature fluid inclusions from Duobuza porphyry copper–gold deposit.

Sample Number	Depth (m)	Lithology	Host minerals	Fluid inclusions types	Salinity (wt% NaCl equiv.)	Homogenization temperature (°C)	Pressure (MPa)
DEJ1-1	Surface	Argillic-silicified granodiorite porphyry	Quartz phenocryst	A, B, C, D, F	48∼73	616∼729	40∼110
			Vein quartz	B	51	683	80
DE1-8	Surface	Silicified-argillic granodiorite porphyry	Quartz phenocryst	A, B, D	34∼56	714∼935	110∼160
			Vein quartz	A, B, C	40∼62	680∼890	60∼160
ZK001-72	72	Potassic-argillic granodiorite porphyry	B-type vein quartz	B	45–54	800∼850	120∼130
ZK002-366	366	Potassic-argillic granodiorite porphyry	Quartz phenocryst	A, B, C	39∼50	729∼857	90∼150
			A-type vein quartz	A, B, D, E, F	40∼61	648∼957	100∼160
ZK0802-225	225	Silicified-propylitic wall rock	Vein quartz	A, C, D	53∼74	650∼850	70∼130

spatial distribution. Five of these samples were further analyzed by microthermometry, SEM-EDS for daughter-mineral analysis and/or Raman spectroscopy. Over 40 fluid inclusions were analyzed by microthermometry. Microthermometric measurements were made in the fluid inclusion laboratory of the Institute of Geology and Geophysics, Chinese Academy of Sciences. Heating experiments were performed using a Linkam THMSG 1500 stage with a measured precision of ±20°C. Freezing experiments were performed using a Linkam THMS 600 fluid inclusion stage with liquid nitrogen cooling (effective range −100 to 600°C). The salinity of fluid inclusions are obtained by the equation of Sterner *et al.* (1988) for inclusions containing halite, and from the H_2O-NaCl-KCl diagram of Roedder (1984) for three-phase inclusions containing halite and sylvite. Pressure is estimated from the P-T diagram of the H_2O-NaCl system (Bodnar *et al.* 1985).

Daughter minerals in fluid inclusions were identified using scanning electron microscope-energy dispersive spectrometry (SEM-EDS) in the SEM laboratory of the Institute of Geology and Geophysics, Chinese Academy of Sciences. SEM-EDS analyses and secondary electron (SEM-SE) images were acquired on carbon-coated quartz fragments at an electron acceleration potentials of 15 kV. Only one vapor-rich fluid inclusion tested by Raman spectroscopy showed detectable CO_2.

Petrography of high-temperature and high-salinity inclusions

High-temperature fluid inclusions are widely distributed in quartz phenocrysts, but relatively rare in the veins (Table 3). These inclusions are very scarce and they are restricted to discrete domains, where they are either isolated or clustered, implying that they are primary fluid inclusions (Roedder 1984). Petrographic observations indicate that there are any coexisting low-salinity, vapor-rich inclusions. The size of the inclusions was always smaller than 25 μm. They are not petrographically distinguishable from abundant brine inclusions showing homogenization temperatures of <600°C. Vapor usually accounts for 20–30% volume of fluid inclusions, liquid for 10–30%, and daughter minerals for 50–60%. The fluid inclusions contain halite and sylvite and commonly additional opaque minerals (Fig. 4) such as chalcopyrite and hematite. Chalcopyrite is identified by its triangle shape (Fig. 5A). Hematite shows a characteristic red color and is insoluble during heating, probably attributed to H_2 loss (Mavrogenes & Bodnar 1994). Sylvite

Table 3 Types and characteristics of fluid inclusions of high temperature from Duobuza porphyry copper–gold deposit*.

Fluid inclusion types	Characters of inclusions at the temperature of 25°C						Homogenization		
	Shape	Phase composition	Phase number	Daughter mineral	Size range(μm)	Occurrence	Behavior	Salinity (wt% NaCl equiv.)	Temperature (°C)
A	Oval, negative crystal shape	L + V + H	3	H	6∼12	Quartz phenocrysts and quartz veins, more in phenocrysts	Vapor disappearance	39.3∼65.5	729∼957
B	Oval, negative crystal shape	L + V + H + Op1 ± (Op2)	3∼4	H, Op	5∼15	Quartz phenocrysts and quartz veins, more in phenocrysts	Vapor disappearance	34.2∼50.5	616∼935
C	Oval, negative crystal shape	L + V + H ± Op ± Hem ± Uns	4∼6	H, Op, Hem, Uns	6∼15	Quartz phenocrysts and quartz veins, more in phenocrysts	Vapor disappearance	49.2∼72.7	652∼761
D	Oval, negative crystal shape	L + V + H + Sy ± Op ± Hem ± Uns	5∼7	H, Op, Hem, Uns, Sy	6∼14	Quartz phenocrysts and quartz veins, more in phenocrysts	Vapor disappearance	43∼82	689∼881
E	Oval, negative crystal shape	L + V	2		8∼15	Quartz phenocrysts	Liquid disappearance		600∼700
F	Oval, negative crystal shape	L + V ± Op (±Uns)	3∼4	Op, Uns	4∼6	Quartz phenocrysts and quartz veins	Vapor disappearance		740∼940

*The fluid inclusions are classified by room temperature, phase composition and behavior of homogeneous patterns. Abbreviations: H, Halite; Sy, Sylite; V, Vapor; Op, Opaque mineral; Uns, Unidentified mineral; Hem, Hematite.

is characterized by its slightly rounded shape and high solubility. Halite forms perfect uncolored cubes. Some inclusions contain unknown transparent minerals (Fig. 4E,F), which mainly occurred as sub-rounded crystals and need further identification. In addition, glassy melt inclusions were also observed in quartz phenocrysts and early quartz-bearing veins. According to the type and number of daughter minerals at room temperature, inclusions are divided into six types as described in Table 3. We used the SEM to identify chalcopyrite, rutile, K-feldspar, and Fe-Mn bearing chloride (Fig. 5), which are also observed in other porphyry copper deposits of the world (Anthony *et al.* 1984; Roedder 1984; Bodnar 1995; Fan *et al.* 1998; Xie *et al.* 2006).

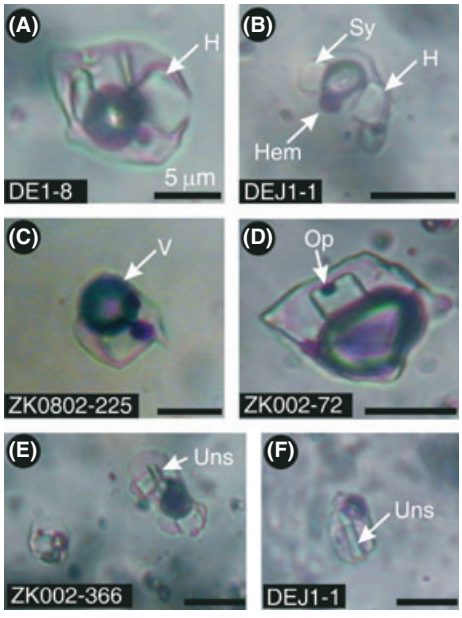

Fig. 4. Types of fluid inclusions with high-temperature and salinity from Duobuza porphyry copper–gold deposit. The fluid inclusions (A, B, E) contain vapor, liquid, and halite, sylvite, opaque mineral, unidentified mineral, hematite. The fluid inclusions (C, D) contain vapor, liquid, and halite, opaque mineral and/or hematite. The fluid inclusion (F) contains vapor, liquid, and unidentified mineral. Abbreviations: H, Halite; Sy, Sylite; V, Vapor; Op, Opaque mineral; Uns, Unidentified mineral; Hem, Hematite.

Halite and sylvite from high-temperature inclusions disappeared early during heating, whereas the vapor disappeared last. Sylvite generally dissolved between 180 and 360°C, followed by halite dissolution between 240 and 540°C. Homogenization through vapor disappearance was observed between 620 and 960°C (Figs 6 and 7). The dissolution temperature of unknown minerals mainly occurred in two temperature ranges, from 550 to 650°C (anhydrite?) and from 850 to 950°C. The latter is higher than the homogenization temperature of fluid inclusions. Hematite is insoluble at 900°C, but its volume becomes smaller. The disappearance temperature of an opaque mineral was measured at about 1030°C.

DISCUSSION AND CONCLUSION

Exsolution of high-temperature and high-salinity fluid

In a homogenization temperature versus salinity (wt% NaCl.equiv) diagram (Figs. 6 and 7), the fluid inclusions plot in a relatively wide salinity range between 34 and 82 wt% NaCl equiv. This is below the halite saturation curve and indicates that the fluid was not saturated with NaCl

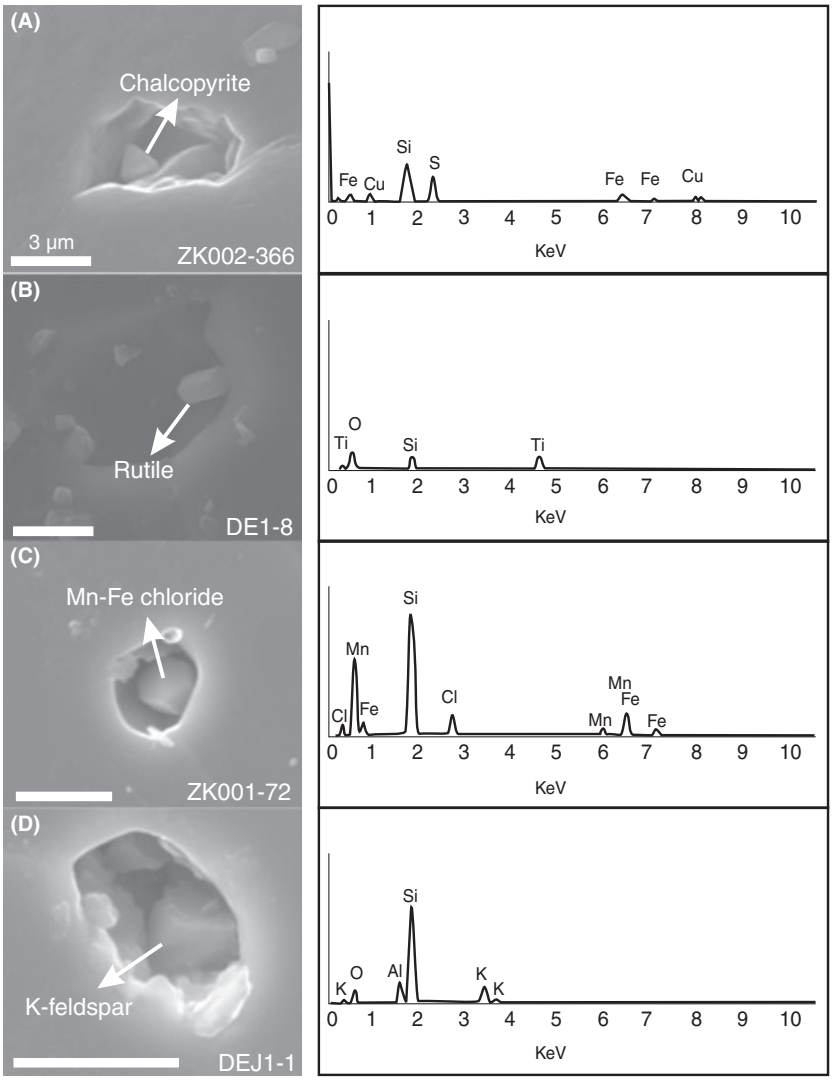

Fig. 5. SEM photomicrographs and EDS spectra of high-temperature and salinity from Duobuza porphyry copper–gold deposit. (A) Chalcopyrite; (B) Rutile; (C) Mn-Fe chloride; (D) K-feldspar.

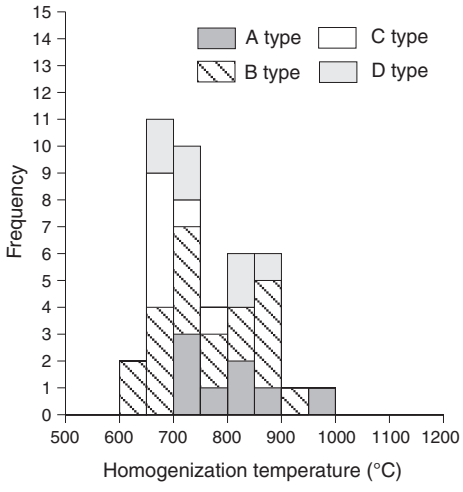

Fig. 6. Histogram of homogenization temperature for all kinds of high-temperature fluid inclusions in the Duobuza porphyry copper–gold deposit.

during trapping. Generally, there are two potential causes for the formation of high-salinity fluid inclusions containing halite in porphyry copper deposits: (i) pressure reduction and phase separation from a low-salinity fluid (Burnham 1979; Hedenquist & Lowenstern 1994; Hedenquist *et al.* 1998; Ulrich *et al.* 2002; Klemm *et al.* 2007; Landtwing *et al.* 2010); (ii) direct exsolution from the magma (Roedder & Coombs 1967; Cline & Bodnar 1991; Lowenstern 1994; Shinohara 1994; Bodnar 1995; Kamenetsky *et al.* 1999; Campos *et al.* 2002, 2006; Veklser 2004; Webster & Mandeville 2007). As there are no low-salinity vapor inclusions coexisting with high-temperature brines in the Duobuza porphyry copper–gold deposit, we suggest that these saline fluids have directly exsolved by magma immiscibility, rather than by later boiling or condensation from a low-salinity fluid. Minimal trapping pressures for fluid inclusions of the Duobuza porphyry copper–gold deposit are estimated between 50 and 160 MPa

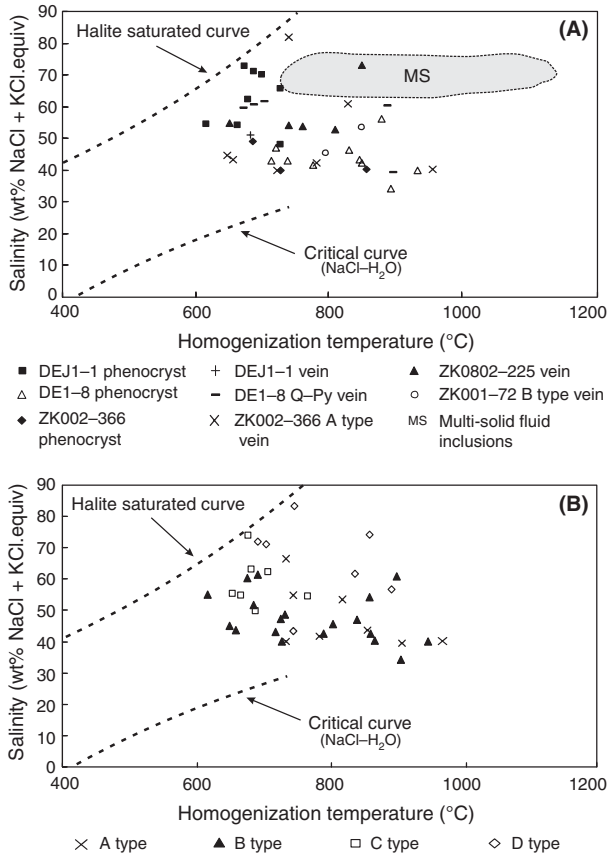

Fig. 7. Homogenization temperature (Th) versus salinity diagram for high-temperature fluid inclusions in Duobuza porphyry copper–gold deposit. (A) Classified by the host mineral quartz; (B) classified by the types of fluid inclusions; (The data of MS fluid inclusion coming from Campos *et al.* 2002).

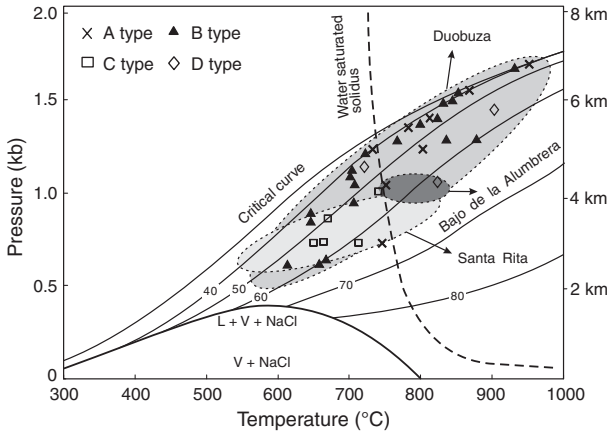

Fig. 8. Temperature versus pressure diagram for high-temperature fluid inclusions in Duobuza porphyry copper–gold deposit (original plot from Bodnar *et al.* 1985). The data of Santa Rita from Reynolds & Beane (1985), Bajo de la Alumbrera from Harris *et al.* (2003). And H_2O-saturated solidus is original from Chou (1987), Critical curve from Sourirajan & Kennedy (1962).

(Fig. 8). Experimental studies have shown that at 700°C and at pressure above 130 MPa, the first exsolved magmatic fluids are single-phase and high-saline fluids, followed by a gradual salinity decrease during magma crystallization (Kilinc & Burnham 1972; Cline & Bodnar 1991; Candela & Piccoli 1995). At intermediate and low pressures (<130 MPa), initial magmatic fluids are of low salinity but gradually increase in salinity with magma crystallization. And the fluid is separating into a low-salinity vapor and a high-salinity brine (Cline & Bodnar 1991; Shinohara 1994; Webster & Mandeville 2007). On the basis of the observation of high-salinity brines only, we interpret that they directly exsolved from the magma at pressures >130 MPa. This minimum pressure is consistent with the experimental stability of a 40 wt% NaCl equiv. fluid homogenizing at 950°C requiring a minimum pressure of about 160 MPa (Fig. 8; Bodnar *et al.* 1985). The salinity of initial exsolving fluid is positively correlated with pressure and Cl/H_2O ratio in the original magma (Cline & Bodnar 1991; Shinohara 1994; Candela & Piccoli 1995; Webster 2004; Webster & Mandeville 2007). The slight increasing salinity with decreasing homogenization temperature (Fig. 7) may be the result of increasing pressure or Cl/H_2O ratio (probably caused by hornblende crystallization; Cline & Bodnar 1991).

A model for magmatic to hydrothermal evolution of fluids at Duobuza

Observations of high-temperature and high-salinity fluid inclusions in combination with published information about intermediate-to-low temperature (≤600°C) fluid inclusions (Li *et al.* 2007) indicate the following fluid evolution in the Duobuza porphyry copper–gold deposit.

(1) At a temperature of 700–1000°C and a minimum pressure of about 110–160 MPa (lithostatic pressure at depth of 4–7 km), the magma reached saturation of a high-salinity magmatic fluid (cf. Cline & Bodnar 1991; Shinohara 1994; Bodnar 1995; Kamenetsky *et al.* 1999; Campos *et al.* 2006; Webster & Mandeville 2007). We cannot exclude the additional presence of a vapor phase, but there is no fluid inclusion evidence for this. The fluid extracted Cu, Au, and other ore-forming elements from the magma.

(2) At a temperature of 600–700°C and a pressure of about 80–100 MPa (lithostatic pressure, depth of around 3∼4 km), the measured homogenization temperature of a vapor-rich inclusion in the ZK002-366 quartz phenocrystal at 697°C is taken to indicate the highest vapor separation temperature (Hedenquist *et al.* 1998).

(3) At 400–600°C and 30–80 MPa (lithostatic pressure, depth of 1∼3 km; Fournier 1999), the magmatic fluid underwent extensive boiling (Li *et al.* 2007). At this

time, the pressure of magma was below the pressure (<130 MPa) required for single-phase fluid exsolution and separated into brine and vapor (Cline & Bodnar 1991; Shinohara 1994). Boiling temperature and pressure decrease and possibly other factors resulted in the precipitation of Cu, Au, and other elements at this stage (Hedenquist & Lowenstern 1994; Hedenquist *et al.* 1998; Redmond *et al.* 2004; Li *et al.* 2007).

(4) At a temperature lower than 400°C and a minimum pressure of about 5–25 MPa (hydrostatic pressure, depth of 0.5–2.5 km), low-salinity aqueous liquid may have formed by cooling and contraction of magmatic vapor (Heinrich *et al.* 2004). This is consistent with the relatively great depth inferred for the deposit (Li *et al.* 2007).

In conclusion, we suggest that the large size and relatively high ore grade of the Duobuza porphyry copper–gold deposit was favored by direct high-temperature exsolution of highly saline magmatic fluids from an oxidized hydrous granodioritic magma. The fluid transferred sulfur and metals from the crystallising melt into lower-temperature veins where ore minerals precipitated.

ACKNOWLEDGEMENTS

This article was funded by Natural Science Foundation Project (40672068, 40902027) and the China Postdoctoral Science Foundation (20090450567). We have obtained support and help from Mr. Zhang Tianping senior geologist and other geologists of the No.5 Geological Team, Tibet Bureau of Geology and Exploration, and obtained specific guidance and assistance from Prof. Lijuan Wang at the Experimental Process of Fluid Inclusions Group in the Institute of Geology and Geophysics, Chinese Academy of Sciences. We were inspired by discussions with Prof. Hongrui Fan. The English text was edited with assistance from Christoph Heinrich and Tobias Schlegel. The manuscript benefited from constructive comments by three Geofluids reviewers, Christoph Heinrich, Philip Candela, and Jake Lowenstern.

REFERENCES

Anthony EY, Reynolds TJ, Beane RE (1984) Identification of daughter minerals in fluid inclusions using scanning electron microscopy and energy dispersive analysis. *American Mineralogist*, **69**, 1053–7.

Audétat A, Pettke T (2003) The magmatic-hydrothermal evolution of two barren granites: a melt and fluid inclusion study of the Rito del Medio and Canãda Pinabete plutons in northern New Mexico (USA). *Geochimica et Cosmochimica Acta*, **67**, 97–121.

Bodnar RJ (1995) Fluid-inclusion evidence for a magmatic source for metals in porphyry copper deposits. In: *Magmas, Fluids and Ore Deposits* (ed. Thompson JFH), pp. 139–52. Short Course Series 23, Mineralogical Association of Canada, Vancouver, BC.

Bodnar RJ, Burnham CW, Sterner SM (1985) Synthetic fluid inclusions in natural quartz. III. Determination of phase equilibrium properties in the system H_2O-NaCl to 1000°C and 1500 bars. *Geochimica et Cosmochimica Acta*, **49**, 1861–73.

Burnham CW (1979) Magma and hydrothermal fluids. In: *Geochemistry of Hydrothermal Ore Deposits* (ed. Barnes HL). 2nd edn. pp. 71–136. Holt, Rinehart and Winston, New York.

Campos E, Touret JLR, Nikogosian I, Delgado J (2002) Overheated, Cu-bearing magmas in the Zaldivar porphyry-Cu deposit, Northern Chile. Geodynamic consequences. *Tectonophysics*, **345**, 229–51.

Campos E, Touret JLR, Nikogosian I (2006) Magmatic fluid inclusions from the Zaldivar deposit, northern Chile: the role of early metal-bearing fluids in a porphyry copper system. *Resource geology*, **56**, 1–8.

Candela PA, Holland HD (1986) A mass-transfer model for copper and molybdenum in magmatic hydrothermal systems – the origin of porphyry-type ore-deposits. *Economic Geology*, **81**, 1–19.

Candela PA, Piccoli PM (1995) Model ore-metal partitioning from melts into vapor and vapor/brine mixtures. In: *Magmas, Fluids, and Ore Deposits* (ed. Thompson JFH), pp. 101–27. Vol. 23. Mineralogical Association of Canada Short Course Series, Ottawa.

Chou I-M (1987) Phase relations in the system NaCl-KCl-H_2O: III. Solubilities of halite in vapor-saturated liquids above 445°C and redetermination of phase equilibrium properties in the system NaCl-H_2O to 1000°C and 1500 bars. *Geochimica et Cosmochimica Acta*, **51**, 1965–75.

Cline JS, Bodnar RJ (1991) Can economic porphyry copper mineralization be generated by a typical Calc-Alkaline melt? *Journal of Geophysical Research*, **5**, 8113–26.

Fan HR, Xie YH, Wang YL (1998) Determining daughter minerals in fluid inclusions under scanning electron microscope. *Geological Science and Technology Information*, **17**(supp), 111–7. (in Chinese with English abstract).

Fournier RO (1999) Hydrothermal processes related to movement of fluid from plastic into brittle rock in the magmatic-epithermal environment. *Economic Geology*, **94**, 1193–211.

Gustafson LB, Hunt JP (1975) The porphyry copper deposit at El Salvador, Chile. *Economic Geology*, **70**, 857–912.

Gustafson LB, Quiroga GJ (1995) Patterns of mineralization and alteration below the porphyry copper orebody at El Salvador, Chile. *Economic Geology*, **90**, 2–16.

Harris AC, Kamenetsky VS, White NC, van Achterbergh E, Ryan CG (2003) Melt inclusions in veins: linking magmas and porphyry Cu deposits. *Science*, **302**, 2109–11.

Hedenquist JW, Lowenstern JB (1994) The role of magmas in the formation of hydrothermal ore deposits. *Nature*, **370**, 519–27.

Hedenquist JW, Arribas AJ, Reynolds TJ (1998) Evolution of an intrusion-centered hydrothermal system: Far Southeast-Lapanto porphyry and epithermal Cu-Au deposits, Philippines. *Economic Geology*, **93**, 373–404.

Heinrich CA (2007) Fluid-fluid interactions in magmatic-hydrothermal ore formation. *Reviews in Mineralogy and Geochemistry*, **65**, 363–87.

Heinrich CA, Driesner T, Stefansson A, Seward TM (2004) Magmatic vapor contraction and the transport of gold from the porphyry environment to epithermal ore deposits. *Geology*, **32**, 761–4.

Heinrich CA, Halter W, Landtwing MR, Pettke T (2005) The formation of economic porphyry copper (-gold) deposits: constraints from microanalysis of fluid and melt inclusions. In: *Mineral Deposits and Earth Evolution* (eds Mcdonald I, Boyce

AJ, Butler IB, Herrington RJ, Polya DA), Geological Society Special Publication, London, Vol. 248, 247–63.

Hou ZQ, Gao YF, Qu XM, Rui ZY, Mo XX (2004) Origin of adakitic intrusives generated during mid-Miocene East-west extension in southern Tibet. *Earth and Planetary Science Letters*, **220**, 139–55.

Imai A (2005) Evolution of hydrothermal system at the Dizon porphyry Cu-Au deposit, Zambales, Philippines. *Resource geology*, **55**, 73–90.

Kamenetsky VS, Kamenetsky MB (2010) Magmatic fluids immiscible with silicate melts: examples from inclusions in phenocrysts and glasses, and implications for magma evolution and metal transport. *Geofluids*, **10**, 293–311.

Kamenetsky VS, Wolfe RC, Eggins SM, Mernagh TP, Bastrakov E (1999) Volatile exsolution at the Dinkidi Cu–Au porphyry deposit, Philippines: a melt-inclusion record of the initial ore-forming process. *Geology*, **27**, 691–4.

Kilinc IA, Burnham CW (1972) Partitioning of chloride between a silicate melt and coexisting aqueous phase from 2 to 8 kilobars. *Economic Geology*, **67**, 231–5.

Klemm LM, Pettke T, Heinbicth CA, Campos E (2007) Hydrothermal evolution of the El Teniente deposit, Chile: Porphyry Cu-Mo ore deposition from low-salinity magmatic fluids. *Economic Geology*, **102**, 1021–45.

Landtwing MR, Furrer C, Redmond PB, Pettke T, Guillong M, Heinrich CA (2010) The Bingham canyon porphyry Cu-Mo-Au Deposit III. zoned copper-gold ore deposition by magmatic vapor expansion. *Economic Geology*, **105**, 91–118.

Li JX (2008a) *Geochronology, Petrology and Metallogeneses of High Oxidized Magma-Hydrothermal Fluid of Duobuza Gold-Rich Porphyry Copper Deposit in Bangonghu belt, Northern Tibet*. Ph.D thesis, Institute of Geology and Geophysics, Chinese Academy of Sciences, p 225 (in Chinese with English abstract).

Li JX, Qin KZ, Li GM (2006) The basic characteristics of gold–rich porphyry copper deposits and their ore sources and evolving processes of high oxidation magma and ore-forming fluid. *Acta Petrologica sinica*, **22**, 678–88. (in Chinese with English abstract).

Li GM, Li JX, Qin KZ, Zhang TP, Xiao B (2007) High temperature, salinity and strong oxidation ore-forming fluid at Duobuza gold-rich porphyry copper in the Bangonghu tectonic belt, Tibet: evidence from fluid inclusions study. *Acta Petrologica Sinica*, **23**, 935–52. in Chinese with English abstract).

Li JX, Li GM, Qin KZ, Xiao B (2008b) Geochemistry of porphyries and volcanic rocks and ore-forming geochronology of Duobuza gold-rich porphyry copper deposit in Bangonghu belt, Tibet: constraints on metallogenic tectonic settings. *Acta Petrologica Sinica*, **24**, 531–43. (in Chinese with English abstract).

Lowenstern JB (1994) Chlorine, fluid immiscibility, and degassing in peralkaline magmas from Pantelleria, Italy. *American Mineralogist*, **79**, 353–69.

Mavrogenes JA, Bodnar RJ (1994) Hydrogen movement into and out of fluid inclusions in quartz – experimental-evidence and geologic implications. *Geochimica Et Cosmochimica Acta*, **58**, 141–8.

Mo XX, Pan GT (2006) From the Tethys to the formation of the Qinghai-Tibet Plateau: constrains by tectono-magmatic events. *Earth Science Frontiers*, **13**, 43–51. (in Chinese with English abstract).

Redmond PB, Einaudi MTI, Nan EE, Landtwing MR, Heinrich CA (2004) Copper deposition by fluid cooling in intrusion-centered systems: new insights from the Bingham Porphyry ore deposit, Utah. *Geology*, **32**, 217–20.

Reynolds TJ, Beane RE (1985) Evolution of hydrothermal fluid characteristics at the Santa Rita, New Mexico, porphyry copper deposit. *Economic Geology*, **80**, 1328–47.

Roedder E (1984) Fluid inclusions. *Reviews in Mineralogy*, **12**, 1–644.

Roedder E, Coombs DS (1967) Immiscibility in granitic melts, indicated by fluid inclusions in ejected granitic blocks from Ascension Island. *Journal of Petrology*, **8**, 417–51.

She HQ, Li JW, Feng CY, Ma DF, Pan GT, Li GM (2006) The high-temperature and hypersaline fluid inclusions and its Implications to the metallogenesis in Duobuza porphyry copper deposit, Tibet. *Acta Geologica Sinica*, **80**, 1434–47. (in Chinese with English abstract).

Shi RD (2007) SHRIMP dating of the Bangong Lake SSZ-type ophiolite: constraints on the closure time of ocean in the Bangong Lake-Nujiang River, northwestern Tibet. *Chinese Science Bulletin*, **52**, 936–41.

Shinohara H (1994) Exsolution of immiscible vapor and liquid phases from a crystallizing silicate melt: implications for chlorine and metal transport. *Geochimica et Cosmochimica Acta*, **58**, 5215–21.

Sourirajan S, Kennedy GC (1962) The system H_2O-NaCl at elevated temperatures and pressures. *American Journal of Science*, **260**, 115–41.

Sterner SN, Hall DL, Bodnar RJ (1988) Synthetic fluid inclusions.V Solubility relations in the system NaCl-KCl-H_2O under vapour-saturated conditions. *Geochimica et Cosmochimica Acta*, **52**, 989–1005.

Ulrich T, Günther D, Heinrich CA (2002) The evolution of a porphyry Cu-Au deposit, based on LA-ICP-MS analysis of fluid inclusions: Bajo de la Alumbrera, Argentina. *Economic Geology*, **97**, 1888–920.

Veklser IV (2004) Liquid immiscibility and its role at the magmatic-hydrothermal transition: a summary of experimental studies. *Chemical Geology*, **210**, 7–31.

Webster JD (1997) Exsolution of magmatic volatile phases from Cl-enriched mineralizing granitic magmas and implications for ore metal transport. *Geochimica et Cosmochimica Acta*, **61**, 1017–29.

Webster JD (2004) The exsolution of magmatic hydrosaline melts. *Chemical Geology*, **210**, 33–48.

Webster JD, Mandeville CW (2007) Fluid immiscibility in volcanic environments. *Reviews in Mineralogy & Geochemistry*, **65**, 313–62.

Xie YL, Yi LS, Xu JH, Li GM, Yang ZM, Yin SP (2006) Characteristics of ore-forming fluids and their evolution for Chongjiang copper deposit in Gangdese porphyry copper belt, Tibet: evidence from fluid inclusions. *Acta Petrologica Sinica*, **22**, 1023–30. (in Chinese with English abstract).

Zhang DH, Zhang WH, Xu GJ (2001) Exsolution and evolution of magmatic hydrothermal fluids and their constraints on the porphyry ore-forming system. *Earth Science Frontiers*, **8**, 194–202. (in Chinese with English abstract).